

# APPLICATION OF LUKÁČ-BALÍK MODEL FOR CHARACTERIZATION OF WORK HARDENING BEHAVIOUR OF Mg-Zn AND Mg-Al ALLOYS

KRISTIAN MÁTHIS<sup>1\*</sup>, ZUZANKA TROJANOVÁ<sup>2</sup>

<sup>1</sup>*Laboratoire GPM2, ENSPG, 101 rue de la Physique, Dom. Univers, BP. 46, 38402 Saint Martin d'Herès, France*

<sup>2</sup>*Department of Metal Physics, Charles University, Ke Karlovu 5, 121 16 Prague 2, Czech Republic*

Received 10 February 2005, accepted 15 April 2005

The Lukáč-Balík model, describing the dislocation density evolution in metallic alloys, was applied for characterization of work hardening behaviour of room temperature deformed magnesium alloys, containing various amounts of aluminium and zinc. The analysis of stress dependences of the work hardening rate predicted by the model has shown that the solute elements strongly influence hardening and softening processes. The Zn addition enhances annihilation of dislocations by cross slip and thereby the ductility at room temperature. On the other hand, Al increases the room temperature strength because of blockage of dislocations moving in basal slip system.

**Key words:** magnesium alloys, plastic deformation, hardening behaviour, dislocation density evolution

## 1. Introduction

Hexagonal structured magnesium alloys have been the focus of interest for many years, especially because of their excellent mechanical properties [1–6]. Their wide industrial application leads to a need for detailed knowledge about their deformation behaviour. The analysis of stress dependence of work hardening curves by means of models worked out by various authors [7–12] could give information about the evolution of dislocation structure and deformation processes during deformation. As was shown in our previous works [13–15], Lukáč-Balík model [11] is the most appropriate for describing deformation behaviour of hexagonal metals.

In the present work, tensile data from the literature [16, 17] for a range of Mg-Al and Mg-Zn solid solutions are analysed by means of Lukáč-Balík model [11] for

---

\*corresponding author, e-mail: mathis@apollo.karlov.mff.cuni.cz

softening and hardening. The role of solute atoms on the deformation behaviour is also discussed.

## 2. Lukáč-Balík model for hardening and softening

Lukáč and Balík's evolution equation of dislocation density [11] is divided into two hardening and two softening components. They assume that the hardening occurs due to the multiplication of dislocations at both impenetrable obstacles and forest dislocations. Dislocation annihilation, due to cross slip and dislocation climb, is considered the dominant softening process. The overall evolution of the dislocation density  $\rho$  with strain  $\varepsilon$  thus can be described as

$$\frac{\partial \rho}{\partial \varepsilon} = K_1 + K_2 \rho^{1/2} - K_3 \rho - K_4 \rho^2, \quad (1)$$

where  $K_1 = 1/bs$ ,  $s$  is the spacing between impenetrable obstacles and  $b$  is the magnitude of the Burgers vector,  $K_2$  is a coefficient of the dislocation multiplication intensity due to interaction with forest dislocations,  $K_3$  and  $K_4$  are coefficients of dislocation recovery intensity due to the cross slip and climb of dislocations, respectively. The stress dependence of the work hardening rate  $\theta$  for polycrystals can thus be written in the form:

$$\Theta = A/(\sigma - \sigma_y) + B - C(\sigma - \sigma_y) - D(\sigma - \sigma_y)^3, \quad (2)$$

where the parameter  $A$  is connected with the interaction of dislocations with the non-dislocation obstacles and is expected to increase with increased solute content or the presence of precipitates of second phase particles; the parameter  $B$  relates to the work hardening due to the interaction with forest dislocations; the parameter  $C$  relates to recovery due to cross slip and the parameter  $D$  is connected with the climb of dislocations.  $\sigma$  represents stress and  $\sigma_y$  is the yield stress.

## 3. Data for analysis

The tensile data for both Mg-Zn and Mg-Al solid solutions were taken from Ref. [16] and [17]. The chemical composition and grain sizes of these alloys are given in Tables 1 and 2. The details of the solution heat treatment can be found in the original papers [16, 17]. Tensile testing was carried out at  $8.3 \times 10^{-4} \text{ s}^{-1}$  at room temperature. The work hardening rate  $\theta$  was obtained from the experimental true stress-true strain data by numerical derivation. The model has been fitted to the  $\theta$ - $\sigma$  curves with the help of the TableCurve<sup>®</sup> program.

Table 1. Chemical composition of the Mg-Zn alloys [16]

Nominal Zn content [at.%]	0.2	0.3	0.4	1	2	3
Zn [at.%]	0.21	0.29	0.40	0.98	1.85	2.66
Grain size [ $\mu\text{m}$ ]	47	41	39	35	35	41

Table 2. Chemical composition of the Mg-Al alloys [17]

Nominal Al content [at.%]	1	2	4	6	8
Al [at.%]	0.87	1.8	3.4	5.2	7.44
Grain size [ $\mu\text{m}$ ]	321	291	209	221	95

#### 4. Results and discussion

The true stress-true strain data for Mg-Zn and Mg-Al alloys are given in the Fig. 1 and Fig. 2, respectively. It can be seen, that the type and concentration of solute elements strongly influences the mechanical properties, particularly the ductility. The active hardening and softening mechanisms during the plastic deformation could be found by means of the model using Eq. (2). By this way also the role of solute elements could be explained.

The stress dependence of the work hardening rate  $\theta$ , calculated from the Mg-Zn experimental curves of Fig. 1, and the behaviour predicted by Eq. (2) are shown in Fig. 3. The experimental and theoretical curves are in good agreement also for Mg-Al alloys. The values of the parameters of best fit for Mg-Zn and Mg-Al alloys are given in Table 3 and Table 4, respectively.

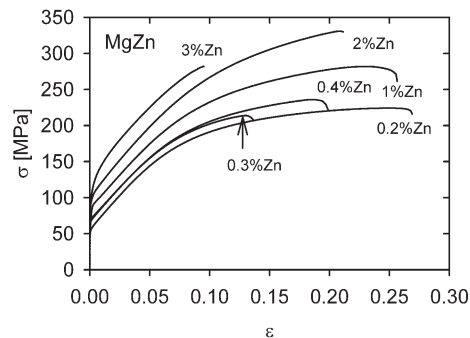


Fig. 1. True stress-true strain curves of Mg-Zn alloys for various Zn contents, adopted from [16].

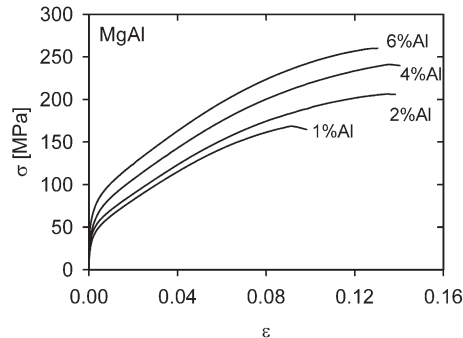


Fig. 2. True stress-true strain curves of Mg-Al alloys for various Al contents, adopted from [17].

The parameter  $A$  increases monotonically with the increasing solute content for both alloys in agreement with the prediction of the model, i.e. the parameter  $A$  is reciprocally proportional to the distance of impenetrable obstacles [11]. The results suggest the increasing role of dislocation – non-dislocation obstacles (e.g. solute atoms, clusters, precipitates, dispersoids) in the hardening mechanism. However, there are two different hardening mechanisms in Mg-Zn and Mg-Al alloys.

Hardening mechanisms in monocrystals of Mg-1.9at.%Zn alloys at low temperatures (4.2–300 K) were investigated by Chun and Byrne [18]. They assumed that hardening takes place by cutting of Zn clusters by dislocations.

This process is energetically favorable due to the lower stacking fault energy of Zn clusters in comparison to that of the Mg matrix [19]. Forming of Zn clusters is supported by migration of dislocation loops [20]. Nevertheless, they did not exclude the existence of other mechanisms.

Cáceres and Blake proposed a different hardening mechanism of Mg-3at.%Zn, deformed at ambient temperature [16]. Their explanation is based on results of

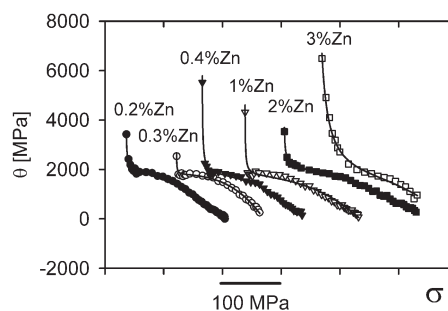


Fig. 3. The symbols represent the work-hardening rate calculated from flow curves of Fig. 1 (Mg-Zn alloys). The solid lines are the lines of best fit according to Eq. (2).

Table 3. Concentration dependence of the parameters of best fit for Eq. (2) and the calculated and measured yield stress for Mg-Zn alloys

	$A$ [MPa <sup>2</sup> ]	$B$ [MPa]	$C$	$D \times 10^4$ [MPa <sup>-2</sup> ]	$R^2$	$\sigma_y$ [MPa]	$\sigma_{02}$ Exp [MPa]
0.2 % Zn	820 ± 180	2010 ± 20	5.4 ± 0.3	2.77 ± 0.07	0.987	57.40 ± 0.10	59
0.3 % Zn	930 ± 60	1750 ± 10	0.5 ± 0.2	4.97 ± 0.05	0.988	71.48 ± 0.07	71
0.4 % Zn	1940 ± 160	1910 ± 20	4.2 ± 0.3	2.30 ± 0.04	0.986	65.76 ± 0.04	70
1 % Zn	1870 ± 170	1780 ± 20	2.7 ± 0.3	1.65 ± 0.06	0.97	87.28 ± 0.06	86
2 % Zn	11100 ± 600	1780 ± 30	1.6 ± 0.3	1.00 ± 0.04	0.984	97.80 ± 0.20	100
3 % Zn	46000 ± 6000	1360 ± 190	3E-3 ± 1.7	1.17 ± 0.28	0.988	114.70 ± 0.10	109

Table 4. Concentration dependence of the parameters of best fit for Eq. (2) and the calculated and measured yield stress for Mg-Al alloys

	$A$ [MPa <sup>2</sup> ]	$B$ [MPa]	$C$	$D \times 10^4$ [MPa <sup>-2</sup> ]	$R^2$	$\sigma_y$ [MPa]	$\sigma_{02}$ Exp [MPa]
1 % Al	23300 ± 1500	1250 ± 80	1.2E-4 ± 1.3	3.0 ± 0.5	0.98	35.1 ± 0.3	40
2 % Al	19800 ± 1500	1340 ± 70	7.7E-4 ± 0.8	2.5 ± 0.2	0.98	43.3 ± 0.4	45
4 % Al	51100 ± 4400	1110 ± 140	1.1E-3 ± 1.3	1.2 ± 0.2	0.96	47.2 ± 0.4	50
6 % Al	64500 ± 5000	1150 ± 150	5.4E-4 ± 0.9	1.0 ± 0.3	0.97	59.1 ± 0.2	60

Sturkey and Clarke [21] acquired in TEM, who described the precipitation of Mg-Zn alloys as follows: in the first step of solidification of solid solution, rod-like Zn precipitates segregate along the crystallographic axis  $c$  and form ordered region. After a certain time these regions transform to the  $\beta'$ -MgZn<sub>2</sub> transient phase or to the MgZn equilibrium phase, eventually. Forming of MgZn<sub>2</sub> phase is energetically favorable in spite of their transient character. Therefore, Cáceres and Blake [16] assumed forming of short range ordered (SRO) regions during solution heat treatment, originating from the transient phase. The calculation of the contribution of SRO to the hardening shows, that SRO is one of the main hardening mechanisms [16].

In the case of Mg-Al alloys neither a transient phase nor SRO regions form owing to the near melting point of the Mg<sub>17</sub>Al<sub>12</sub> intermetallic phase and the surrounding eutectic (difference of 5 °C, contrary to the 250 °C difference of Mg-Zn system), and due to the higher solubility of Al in Mg (Al in Mg: 11.5 at.%, Zn in Mg: 2.4 at.% [1]). Therefore solid solution hardening in the basal plane should be taken into account, as shown by numerous authors [17, 22, 23].

The *parameter B* remains nearly constant for all concentrations for both types of alloys. Since this parameter is connected with the dislocation – forest dislocation interaction, this result indicates that the dislocation density in non-basal slip systems does not change with increasing solute content.

There is a significant difference in *parameter C* of Mg-Zn and Mg-Al alloys, which characterizes the cross slip of screw dislocations. Cross slip most probably takes place through prismatic slip system [24], and an increased activity of this slip system could enhance the ductility. In the case of Mg-Zn alloys, values of parameter  $C$  are of the order assumed by the model and suggest the importance of cross slip in the deformation process. The concentration dependences of this parameter and the ductility are in agreement, i.e. decrease with increasing concentration of Zn,

thus the probability of cross slip decreases as well. It seems that 2 at.% Zn is a critical concentration; above that Zn content ceases improving the slip in prismatic slip system. Similar concentration dependence of prismatic slip system activity was observed also for Zn single crystals [25]. It is necessary to remark that the model is able to describe drop in ductility for 0.3 at.% Zn, where the value of parameter  $C$  is small. This result supports the hypothesis of Akthar and Teghsoonian [22], who assumed a hardening in prismatic plane for this concentration of Zn.

The negligible value for  $C$  in Mg-Al alloys suggests that the addition of Al to Mg does not enhance the cross slip of dislocations. The low incidence of cross slip is in agreement with the neutron diffraction study of AZ31 alloy by Agnew et al. [26] who found a marginal importance of non-basal slip to the macroscopic strain for strains up to 10 %. A negligible role of non-basal system activity up to 200 °C in pure Mg and AZ91 was also found by X-ray diffraction profile analysis [27, 28]. Therefore the main deformation mechanism in Mg-Al alloys is twinning, as it was shown in our previous work [29].

Decreasing of *parameter D* with increasing solute content is most probably connected with reduced climb ability because of the high concentration of solute atoms along the dislocation line, and due to the lowering of the stacking fault energy as the solute content increases. Lowering of stacking fault energy improves the twinning activity as well.

## 5. Conclusions

In the present paper the stress dependence of the work hardening rate of Mg-Zn and Mg-Al alloys was analysed using Lukáč-Balík model. The deformation behaviour of alloys strongly depends on solute type and content. The hardening is a result of dislocation interaction with atoms in solid solution and other dislocations, respectively. The annihilation of dislocations due to the cross slip is the dominant softening mechanism in Mg-Zn alloys. On the other hand, Al addition inhibits cross slip. An additional softening mechanism is annihilation due to the dislocation climb. The climb ability decreases with increasing solute content.

## Acknowledgements

The paper is dedicated to Prof. RNDr. Pavel Lukáč, DrSc., Dr.h.c. on the occasion of his 70<sup>th</sup> birthday. This work was supported by the Grant Agency of the Academy of Sciences of the Czech Republic under grant A2041203.

## REFERENCES

- [1] ASM Speciality Handbook Magnesium and Magnesium Alloys. Eds.: Avedesian, M. M., Baker, H. Materials Park, OH, ASM International 1999.
- [2] TROJANOVÁ, Z.—LUKÁČ, P.: Kovove Mater., 43, 2005, p. 73.
- [3] LAMARK, T. T.—CHMELÍK, F.—ESTRIN, Y.—LUKÁČ, P.: Kovove Mater., 42, 2004, p. 293.

- [4] JÄGER, A.—LUKÁČ, P.—GÄRTNEROVÁ, V.: Kovove Mater., 42, 2004, p. 165.
- [5] TROJANOVÁ, Z.—GÄRTNEROVÁ, V.—PADALKA, O.: Kovove Mater., 42, 2004, p. 206.
- [6] MÁTHIS, K.—MUSSI, A.—TROJANOVÁ, Z.—LUKÁČ, P.—RAUCH, E.: Kovove Mater., 41, 2003, p. 293.
- [7] KOCKS, U. F.: J. Eng. Mater. Tech., 98, 1976, p. 76.
- [8] ESTRIN, Y.—MECKING, H.: Acta Metall., 32, 1984, p. 57.
- [9] KOVÁCS, I.—CHINH, N. Q.—KOVÁCS-CSETÉNYI, E.: Phys. Stat. Sol. (a), 194, 2002, p. 3.
- [10] MALYGIN, G. A.: Phys. Stat. Sol. (a), 119, 1990, p. 423.
- [11] LUKÁČ, P.—BALÍK, J.: Key Eng. Mater., 97–98, 1994, p. 307.
- [12] CHINH, N. Q.—HORVÁTH, Gy.—HORITA, Z.—LANGDON, T. G.: Acta Mater., 52, 2004, p. 3555.
- [13] MÁTHIS, K.—TROJANOVÁ, Z.—LUKÁČ, P.: Mater. Sci. Eng. A, 324, 2002, p. 141.
- [14] MÁTHIS, K.—TROJANOVÁ, Z.—CÁCERES, C.—LUKÁČ, P.—LENDVAI, J.: J. Alloys & Compounds, 378, 2004, p. 176.
- [15] LUKÁČ, P.—MÁTHIS, K.: Kovove Mater., 40, 2002, p. 281.
- [16] CÁCERES, C. H.—BLAKE, A.: Phys. Stat. Sol. (a), 194, 2002, p. 147.
- [17] CÁCERES, C. H.—ROVERA, D. M.: J. Light Metals, 1, 2001, p. 152.
- [18] CHUN, J. S.—BYRNE, J. G.: J. Mat. Sci., 4, 1969, p. 861.
- [19] HIRSCH, P. B.—KELLY, A.: Phil. Mag., 12, 1965, p. 881.
- [20] CLARK, J. B.: Acta Metall., 13, 1965, p. 1281.
- [21] STURKEY, L.—CLARK, J. B.: J. Inst. Metals, 88, 1959, p. 177.
- [22] AKTHAR, A.—TEGHTSOONIAN, E.: Trans. JIM, 9, 1968, p. 692.
- [23] AKTHAR, A.—TEGHTSOONIAN, E.: Phil. Mag., 25, 1972, p. 897.
- [24] LUKÁČ, P.: In: 3rd International Magnesium Conference. Ed.: Lorimer, G. W. London, The Institute of Materials 1997, p. 516.
- [25] LUKÁČ, P.: Czech. J. Phys., B 31, 1981, p. 135.
- [26] AGNEW, S. R.—TOMÉ, C. N.—BROWN, D. W.—HOLDEN, T. M.—VOGEL, S. C.: Scripta Mater., 48, 2003, p. 1003.
- [27] MÁTHIS, K.—NYILAS, K.—AXT, A.—DRAGOMIR-CERNATESCU, I.—UNGÁR, T.—LUKÁČ, P.: Acta Mater., 52, 2004, p. 2889.
- [28] MÁTHIS, K.—GUBICZA, J.—NAM, N. H.: J. Alloys & Compounds (in press).
- [29] MÁTHIS, K.—CHEMLÍK, F.—TROJANOVÁ, Z.—LUKÁČ, P.—LENDVAI, J.: Mater. Sci. Eng. A, 387–389, 2004, p. 331.